Electronic Supplementary Material (ESI) for Journal of Materials Chemistry A

$MoSe_2$ Nanosheets and Their Graphene Hybrids: Synthesis, Characterizations and Hydrogen Evolution Reaction Studies.

Hao Tang [a], Kunpeng Dou [b], Chao-Cheng Kaun [b], Qing Kuang [a], Shihe Yang[a]*

[a] Department of Chemistry, The Hong Kong University of Science and Technology, Hong Kong

[b] Research Center for Applied Sciences, Academia Sinica, Taipei 11529, Taiwan

Supporting Information

Materials and Methods.

Synthesis and Preparation. We report a facile way to prepared $MoSe_2$ and $MoSe_2$/RGO by hydrothermal reaction followed by low temperature crystallization annealing. All of the chemicals used in the present work were of analytical grade, and the reactions were carried out under open-air conditions using distilled water. Selenium (99.99%), Na_2MoO_4 (99.99%) and hydrazine hydrate ($N_2H_4H_2O$, 98%) solution were obtained from Sigma-Aldrich.

For the preparation of $MoSe_2$ nanosheets: 0.002 mol Na_2MoO_4 was dispersed in 50ml distilled water under constant stirring to form a clear solution. In a separate flask, the required amount of Se powder (0.004mol) was dissolved in hydrazine hydrate solution (10 ml) in open air. Instantly the colorless solution turns dark brown and remains unchanged under atmospheric conditions at least for one day. Then 10ml hydrazine hydrate-Se was added to 50ml Na_2MoO_4 slowly at room temperature. The mixture gives a clear orange-red solution with the final Mo: Se mole ration is about 1:2. Then the mixture was transferred to a 100 mL Teflon-lined autoclave and heated in an oven at 200℃ for 10 h with no intentional control of ramping or cooling rate. The black precipitates was collected by centrifugation at 7000 rpm for 5 min, washed with DI water and recollected by centrifugation. The washing step was repeated for at least 3 times. Then product was dry-vacated overnight. Finally, the precipitates were annealed at 470 °C in flowing high-pure N_2 atmosphere for 10 h to yield final crystalline products.

For the preparation of $MoSe_2$ /RGO nanosheets: GO was made by a modified Hummers method. Then 0.1g GO was dispersed in 50ml distilled water with 0.0005 mol Na_2MoO_4 under constant sonication at room temperature for approximately 30 min until a clear and homogeneous solution was achieved. In a separate flask, 0.001mol Se powder was dissolved in hydrazine hydrate solution (10 ml) in open air. The following steps are similar to those of

preparation of MoSe2 nanosheets. For comparison, the other two $MoSe_2$ /RGO hybrids with different graphene and MoSe2 ratios were prepared: One is with 0.001 mol Na_2MoO_4 and 0.002mol Se, and the hydrothermal reaction time maintained at 10h; and the other is with 0.00025mol Na2MoO4 and 0.0005mol Se, and the hydrothermal reaction time shortened to 6h.

Characterizations. Powder X-ray diffraction (XRD) measurements were carried out using a Philips X'Pert powder diffractometer with Cu KR radiation (λ = 1.54056 A °) with a scan step of 0.05 deg/s. To record the pattern, nanoparticle powder was coated on a glass plate. Scanning electron microscopy (SEM) images were recorded on a JSM 6300 (JEOL). Samples were prepared by drop-drying from an ethanol suspension of the hybrid onto Si wafers. Transmission electron micrographs (TEM), high-resolution transmission electron microscopy (HRTEM) images were recorded using a JEOL JEM-2010 electron microscope at 200 kV. Samples were prepared by drop-drying a diluted suspension of the samples in ethanol onto a 200 mesh holey carbon copper grid that was dried completely under ambient conditions before the measurements. X-ray photoelectron spectroscopy (XPS) spectrum was collected on PHI 5600 (Physical Electronics) XPS Spectrometer. Raman spectrum of powder samples were recorded on LabRAM HR Raman microscope with a laser excitation wavelength of 633 nm. Samples were dispersed on Si (100) wafer with Si Raman mode at 520 cm^{-1} as reference.

Electrochemical Studies. The measurements process is similar to that of MoS_2/graphene described detailed in the previous report [5] for comparison.$MoSe_2$ and $MoSe_2$/RGO electrode fabrication: 4mg catalysts($MoSe_2$ or $MoSe_2$/RGO) was suspended in stock solution containing 0.8mL deionized H_2O, 0.2mL ethanol and 80 μL nafion solution (5%) by ultra-sonication for 30

min to form a homogeneous ink. Then 5 μl of the catalyst ink was drop-casted on rotating glassy carbon electrode of 2 mm in radius (loading ~ 0.16 mg/cm^2) for air drying.

For testing durability, $MoSe_2$/RGO catalyst was loaded onto FTO electrode. The 11 μl of the catalyst ink was drop-casted onto 0.283cm^2 FTO electrode surface (loading ~ 0.156 mg/cm^2), air-dried and subsequently dried in a vacuum oven for hours before use. By doing so, we obtained a $MoSe_2$/RGO/FTO electrode with a similar mass catalyst loading to that of the catalyst on carbon glassy electrode.

Electrochemical analysis was done using a CHI660B. Three electrodes configuration was employed. The working electrode was the glassy carbon electrode with $MoSe_2$ or $MoSe_2$/RGO on it(In stability test, the working electrode was FTO electrode with $MoSe_2$/RGO on it) , the reference electrode was saturated calomel electrode and the counter electrode was a graphite rod. Linear sweep voltammetry (using the pontentiostat from CH Instruments) with scan rate of 5 mVs−1 was conducted in 0.5 M H_2SO_4. In all measurements, we used saturated calomel electrode (SCE) as the reference. It was calibrated with respect to reversible hydrogen electrode (RHE). The calibration was performed in the high purity H_2 saturated electrolyte with a Pt wire as the working electrode. CVs were run at a scan rate of 1 mV s^{-1}, and the average of the two potentials at which the current crossed zero was taken to be the thermodynamic potential for the hydrogen electrode reactions. In 0.5 M H_2SO_4, E (RHE) = E (SCE) + 0.271 V. All the potentials reported in our manuscript are against RHE.

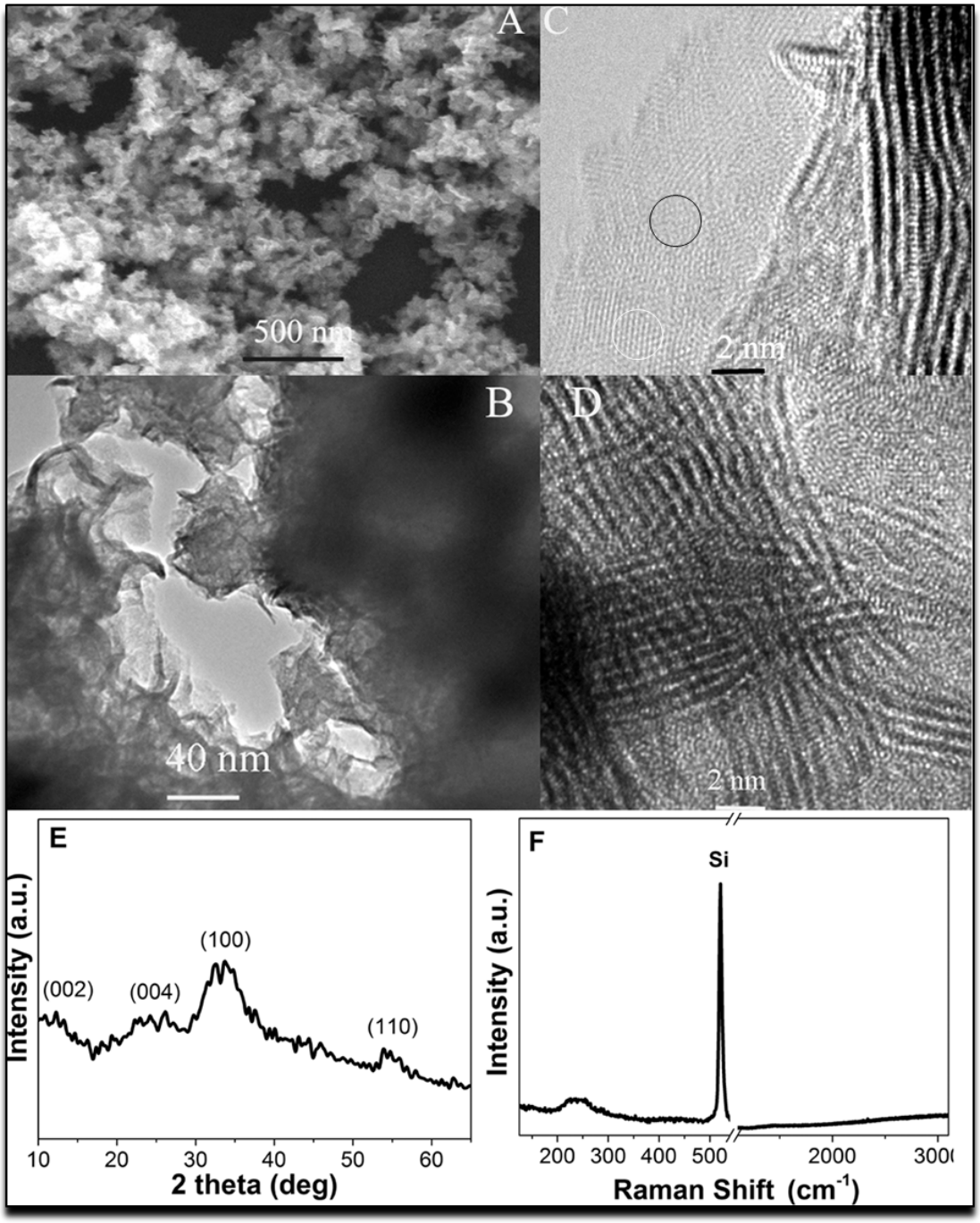

Figure S1. $MoSe_2$ nano-flowers before thermal annealing. (A) SEM image of the $MoSe_2$ nano-flowers. (B) TEM image showing that $MoSe_2$ nano-flowers are composed by ultra-thin nanosheets. (C) HRTEM image showing the side of nanosized $MoSe_2$ with few layers. The $MoSe_2$ nano-flowers are of partial crystallinity (as shown in white circle) with amorphous part

(in black circle). (D) HRTEM image showing the center of nano-size $MoSe_2$, which demonstrate typical folded edges with (002) plane of 2H-$MoSe_2$. (E) XRD pattern shows broad peaks with maxima approximately locating at (002), (004), (100) and (110) of 2H-$MoSe_2$.The broad peaks indicates it is of poor crystalline. (F) Raman spectrum of $MoSe_2$ nanosheets. A_{1g} and E^1_{2g} modes of 2H-$MoSe_2$, which should been in the range 240- 290 cm^{-1}, cannot be detected, while replacing by a broad Raman mode peak. This indicates poor crystalline of $MoSe_2$.

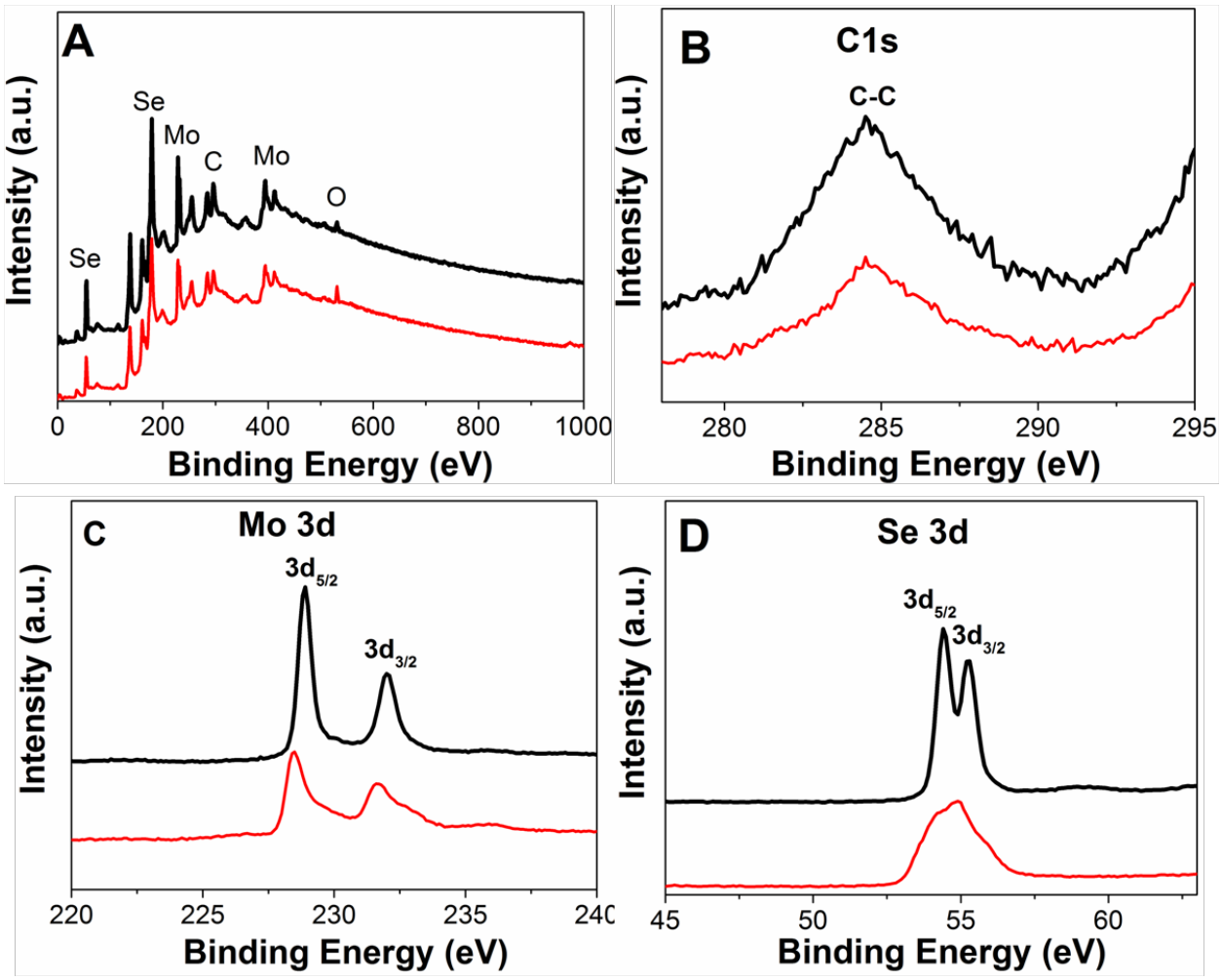

Figure S2. XPS of $MoSe_2$ nanosheets before ( ) and after annealing ( ). (A) Survey spectrum. (B) High resolution C 1s spectrum. (C) High resolution Mo 3d spectrum. (D) High resolution Se 3d spectrum. The small amount of carbon in pure $MoSe_2$ is resulting from precursor or

contaminants during experiment process from environments. To the amorphous sample directly from hydrothermal reaction, the 3d peak of Se is not so well split and molybdenum is in its mix states.

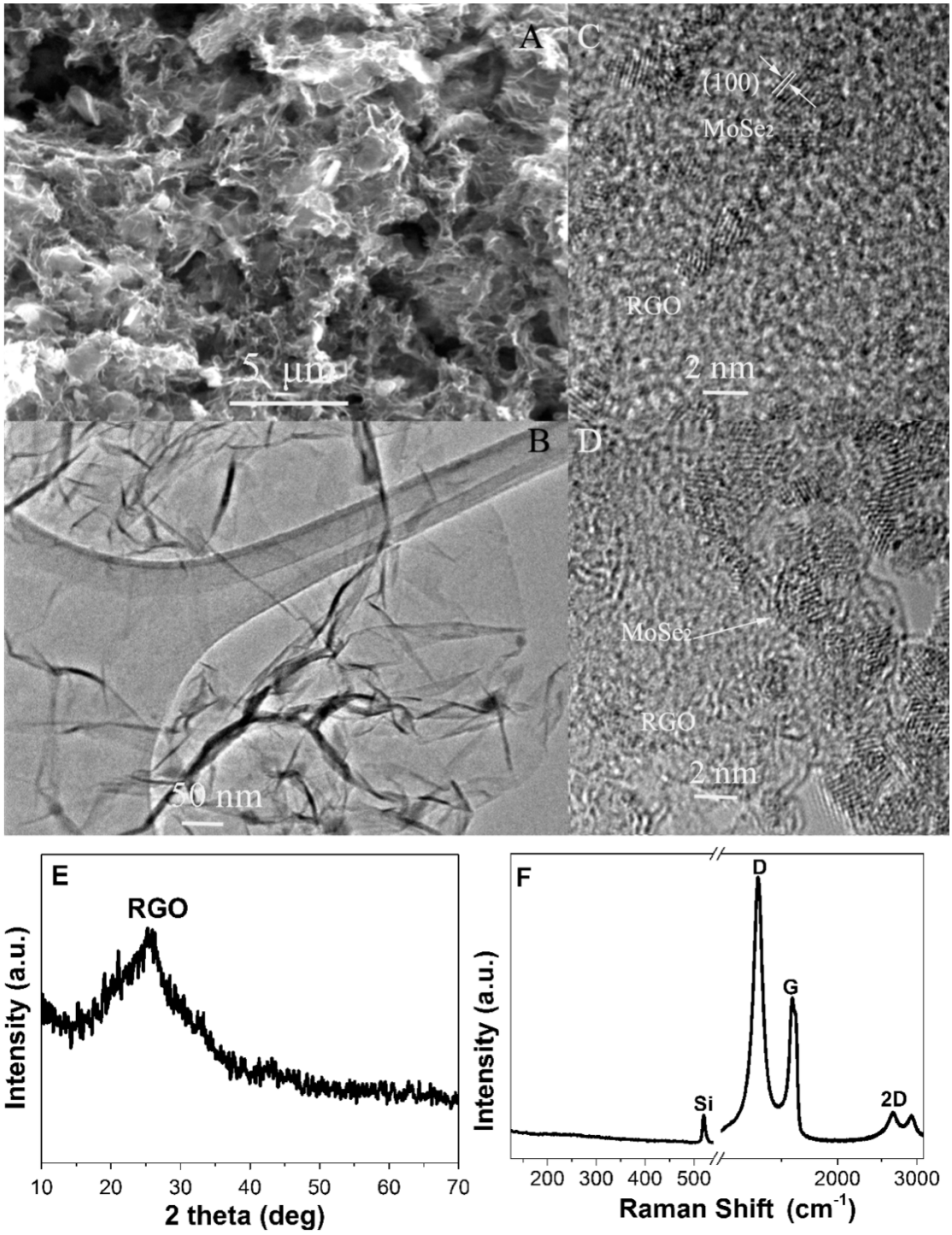

Figure S3. $MoSe_2$/RGO hybrids (sample 2: C: Mo: Se=77:1:1.5) (A) SEM image of the $MoSe_2$/RGO hybrids. (B) TEM image showing the morphology of $MoSe_2$/RGO hybrids. (C) HRTEM image showing $MoSe_2$ nanosheets sparsely stacking on a RGO. (D) HRTEM image showing the density of $MoSe_2$ nanosheets is a little higher on the side of RGO. (E) XRD pattern and (F) Raman spectrum of the hybrid. No $MoSe_2$ XRD and Raman mode peak can be detected for its ultra-low content.

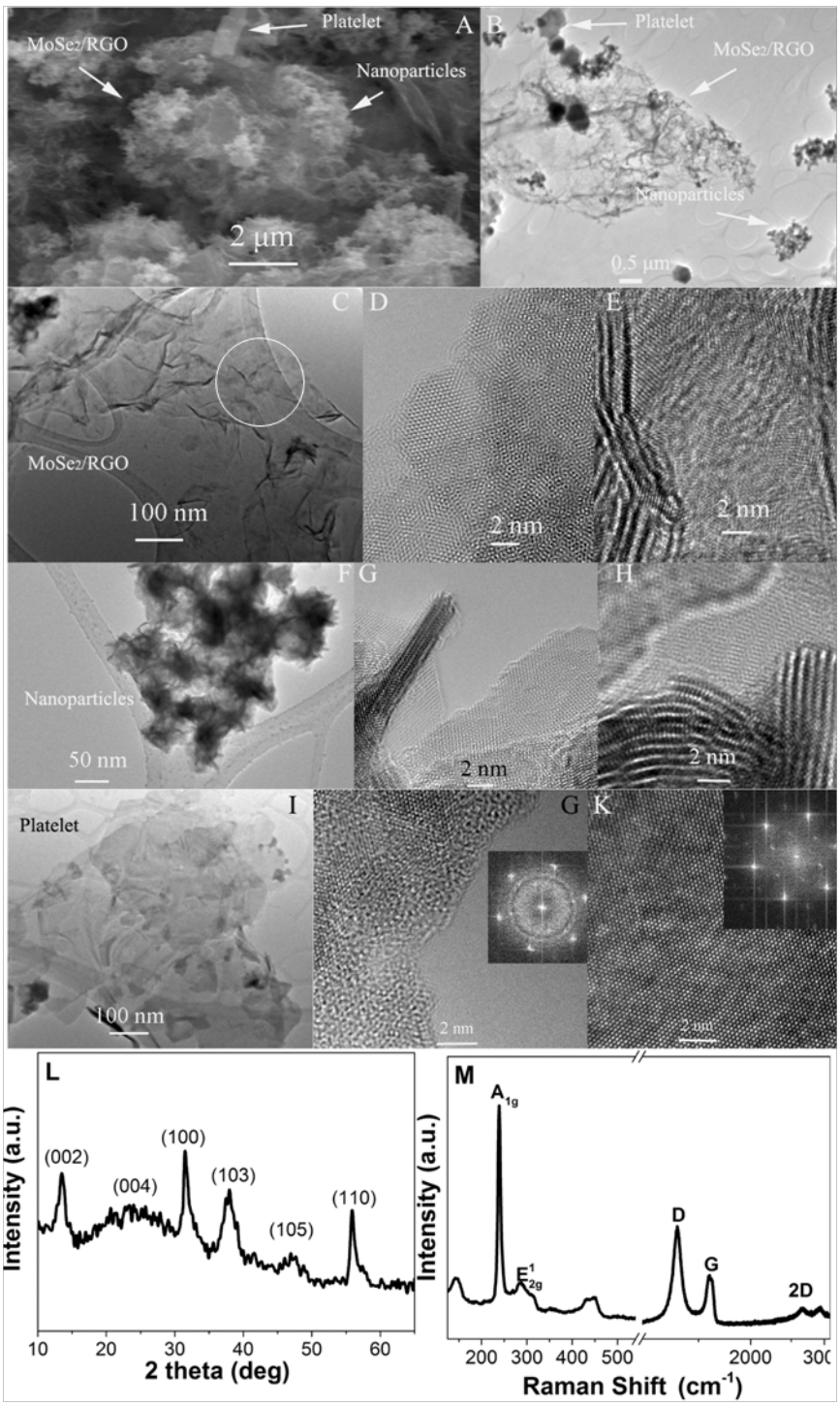

Figure S4. $MoSe_2$/RGO hybrids (sample 3: C: Mo: Se=5:1:2) (A) SEM image and (B) TEM image showing that three kinds of products: $MoSe_2$/RGO hybrids, free $MoSe_2$ nanoparticles and large hexagonal platelets. (C) TEM image of $MoSe_2$/RGO hybrids. Large $MoSe_2$ can be detected in white circle. (D) HRTEM image showing $MoSe_2$ basal plane on a RGO. (E) HRTEM image

showing the hexagonal $MoSe_2$ nanosheets are near to completely cover on surface of RGO. (F) TEM image of pure $MoSe_2$ nano-flowers. (G) HRTEM image showing ultra thin $MoSe_2$ nanosheets with folded edges. (H) HRTEM image showing the center of $MoSe_2$ nanoflowers which were also composed by few layers nanosheets. (I) TEM image of large $MoSe_2$ hexagonal nanoplatelets. (J) HRTEM image showing the side of $MoSe_2$ hexagonal platelets indicating that actually $MoSe_2$ still grows on RGO. Inset is the diffraction pattern which indicates that $MoSe_2$ are single crystal. (K) HRTEM image showing center of $MoSe_2$ nanoplatelets. Inset is the diffraction pattern which indicates it is high quality single crystal. (L) XRD pattern demonstrates it maintains 2H-$MoSe_2$. (M) Raman spectrum of the hybrid.

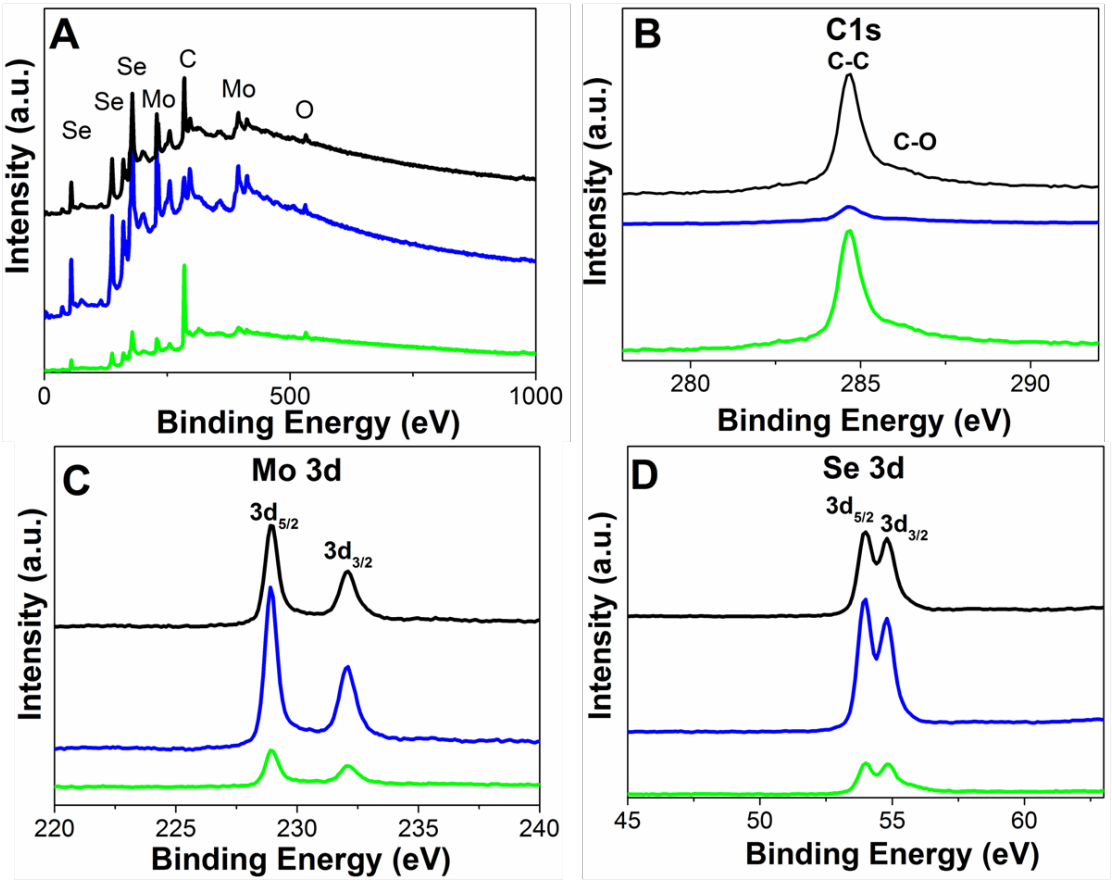

Figure S5. XPS of $MoSe_2$/RGO hybrids(C: Mo: Se=13:1:2; C: Mo: Se=5:1:2; C: Mo: Se=77:1:1.5). (A) Survey spectrum. (B) High resolution C 1s spectrum. (C) High resolution Mo 3d spectrum. (D) High resolution Se 3d spectrum.

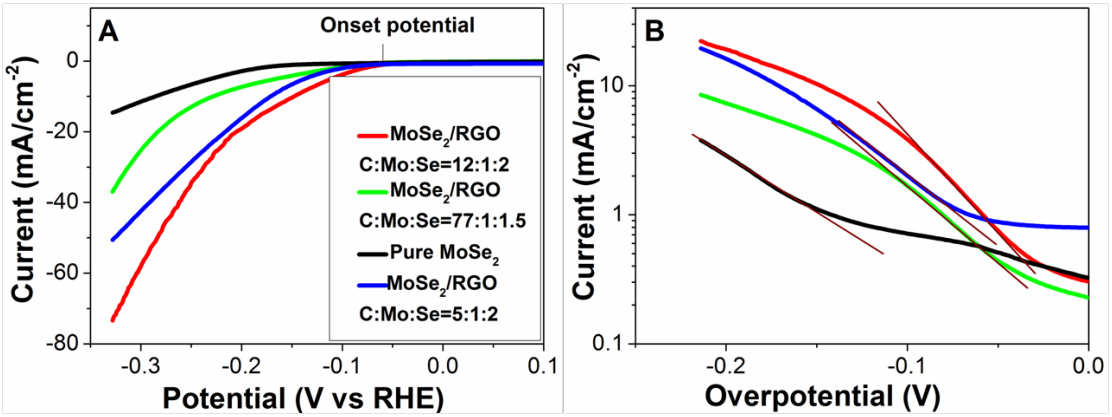

Fig S6. Electrochemical measurements in a cathodic potential window. (A) Polarization curves and (B) corresponding tafel plots recorded on glassy carbon electrodes with a catalysts loading of 0.16 mg/cm^2. Conditions: potential scan rate of 5 mV s-1, electrode rotating rate of 2400 rpm. Pure $MoSe_2$, $MoSe_2$/RGO (C: Mo: Se=13:1:2), $MoSe_2$/RGO (C: Mo: Se=77:1:1.5), $MoSe_2$/RGO (C: Mo: Se=5:1:2)

In sharp contrast, $MoSe_2$/RGO hybrids (sample 1: C:Mo: Se=13:1:2)exhibited even lower onset potential at 0.0.05 V vs. RHE with a tafel slop close to ~69 mV per dec. On one extreme, to the $MoSe_2$/RGO hybrids with C:Mo: Se =77:1:2, onset potential is a little increased to ~0.06 V and tafel slope to ~85 mV/decade; in the other extreme, to the final product with mole ratio C: Mo: Se=5:1:2, where the products include $MoSe_2$ grown on RGO, free $MoSe_2$ and large single crystal $MoSe_2$/RGO heterojunction platelets, the onset potential is increased to ~0.075 V vs. RHE and the tafel slope ~91 mV/decade, approaching those of the pure $MoSe_2$ nano-flowers.

The variance of HER properties of in $MoSe_2$/RGO hybrids are close related to their morphologies and structures and further decided by the growth mechanisms[1]: At low supersaturations of precursor as sample 2, heterogeneous nucleation of $MoSe_2$ nanosheets on GO is predominant. The resulting $MoSe_2$ content is low, and only few nanoparticles formed on RGO with limited active edges contributing to hydrogen generation. When effective content increased, the nanosheets on RGO began to grow up with relative large size and the density was also increased, which all increase the amount of active edges and therefore contributing to overpotential and tafel slop. However, when the precursor content is further increased and at high supersaturations, the homogeneous nucleation, which is the up-limit of heterogeneous nucleation works together with heterogeneous nucleation. Pure $MoSe_2$ nanoparticles can form altogether with $MoSe_2$/RGO hybrid. And the HER property is close to pure $MoSe_2$.

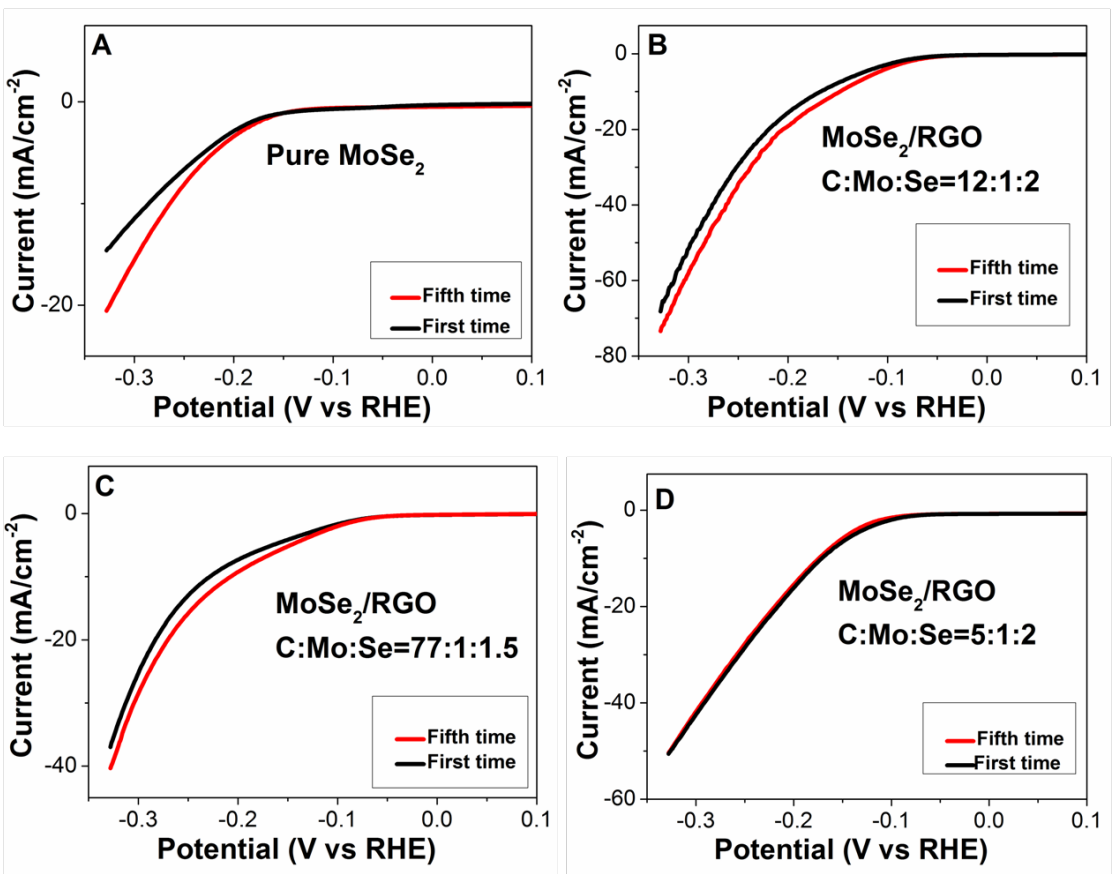

Figure S7. Catalyst stability tests for $MoSe_2$ (A) and $MoSe_2$/RGO (B: C: Mo: Se=13:1:2; C: C: Mo: Se=77:1:1.5; D: C: Mo: Se=5:1:2), in which HER currents are maintained after 50 cycles in the cathodic potentials windows.

.

Computational Methods

The density functional theory calculations have been performed using RPBE2 functional as implemented in VASP package.3 The cutoff energy for the plane wave basis was 420 eV. All atoms were relaxed until the Hellmann-Feynman forces acting on them were below 0.02 eV/Å. A slab model is employed to calculate the hydrogen adsorption energies, which consisting of four Mo atoms in x-direction and six Mo atoms in y-direction based on previous study.4 The lattice constant of MoSe2 has been determined to be 3.347Å and compares well with the experimental lattice constant of 3.299Å. 5 The unit cell dimension in x-direction is 13.388 Å, in y-direction 25Å and in z-direction 18Å. A 4×1×1 Monkhorst-Pack k-point mesh is used for the Brillouin zone sampling. The stability of hydrogen can be described by the differential hydrogen adsorption energyΔE_H which is calculated as follows: [4]

$\Delta E_H = E(MoSe_2+nH) - E(MoSe_2+(n-1)H) - 1/2\ E(H_2)$ (1)

Where E ($MoSe_2$+nH) is the total energy for the $MoSe_2$ slab system with n hydrogen atoms adsorbed on the edge, E ($MoSe_2$+ (n-1) H) is the total energy for (n-1) hydrogen atoms adsorbed on the edge and E (H_2) is the energy for a hydrogen molecule in the gas phase. The differential hydrogen binding energy describes the energy needed to increase the coverage by one hydrogen atom. The slab models with different hydrogen coverages 25% (S1), 50%(S2), 75% (S3) and 100% (S4) are shown in Figure S8. The differential binding energy is defined such that the value for 50% indicates, how much energy is required to increase the coverage from 25% to 50%, and similar for the other coverages.[3] The calculated results show -0.646 eV for 25%, -0.613 eV for 50%, -0.389eV for 75% and 0.045eV for 100%. Based on these energies we calculate the Gibbs free energy for hydrogen adsorption as[3]

$\Delta G_H^0 = \Delta E_H + \Delta E_{ZPE} - T\Delta S_H$ (2)

Where ΔE_H is the differential hydrogen chemisorption energy from formula (1), ΔE_{ZPE} is the difference in zero point energy between the adsorbed state and the gas phase and ΔS_H is the entropy difference between the adsorbed state and the gas phase. The entropy of hydrogen adsorption is taken as $\Delta S_H \cong \frac{1}{2} S^0_{H_2}$ where $S^0_{H_2}$ is the entropy of H_2 (2179.3cm^{-1} for H_2 taken from Ref. 6.) in the gas phase at standard conditions. The calculated vibrational frequencies of H adsorbed on $MoSe_2$ are 2283cm^{-1}, 406cm^{-1} and 348 cm^{-1} for $MoSe_2$ slab with 25% H coverage, 2263cm^{-1}, 532cm^{-1} and 439cm^{-1} for $MoSe_2$ slab with 50% H coverage, 2182cm^{-1}, 436cm^{-1} and 294cm^{-1} for $MoSe_2$ slab with 75% H coverage, 2161cm^{-1}, 559cm^{-1} and 379cm^{-1} for $MoSe_2$ slab with 100% H coverage. Thus we obtain $\Delta G^0_H = \Delta E_H + 0.256$ eV for 25%, $+0.268$ eV for 50%, $+0.249$ eV for 75%, + 0.26eV for 100%. After correction, the differential binding free energies are -0.39 eV for 25%, -0.344 eV for 50%, -0.14 eV for 75% and 0.305eV for 100%. The free energy closest to thermoneutral is -0.14 eV, which describes the coverage at 75%. It is most likely that the hydrogen evolution is mainly driven by hydrogen adsorption at these two coverages.

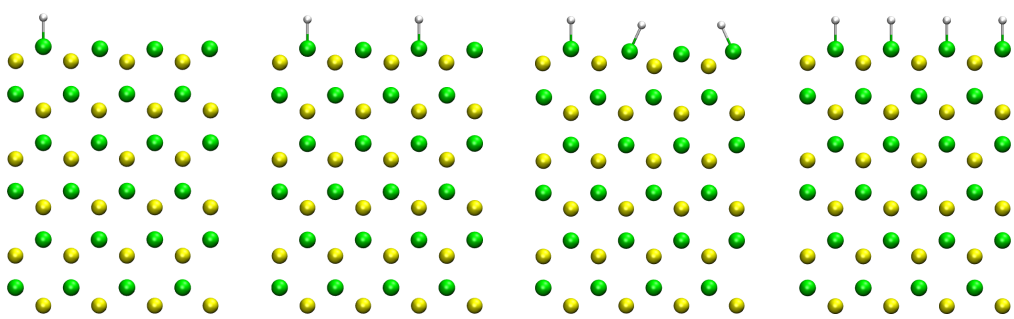

S1 S2 S3 S4

Figure S8. The optimized geometry of MoSe2 slab system with different hydrogen coverages: 25%(S1), 50%(S2), 75%(S3) and 100%(S4). The H, Mo and Sn atoms are represented by the white, green and yellow balls, respectively.

To check the reliability of the above methods, test calculations have been performed for MoS_2 system. The lattice constant of MoS2 has been determined to be 3.207Å and compares well with the experimental lattice constant of 3.16Å[4] and calculated result 3.235Å.[3] The differential hydrogen binding energies are -0.557 eV for 25%, -0.475 eV for 50%, 0.068 eV for 75% and 0.66 eV for 100%. After correction by equation (2), we obtain the differential binding

free energies -0.32eV for 25%, -0.231 eV for 50%, 0.307eV for 75% and 0.909 eV for 100%. The free energy closest to thermoneutral is -0.231 eV, which corresponds to coverage at 50%. Therefore, it is most likely that the hydrogen evolution is mainly driven by hydrogen adsorption at these two coverages. This is acceptable qualitative agreement with the literature [ref 3] which ensure the reliability of methods and results here.

The calculation results of $MoSe_2$ and MoS_2 using same methods provide us the opportunities to compare the HER catalytic activities. The Gibbs free energy for atomic hydrogen adsorption (DGH) on $MoSe_2$ edges is closer to thermoneutral than that of MoS_2, with an H coverage is about 75% on the edge under operating conditions, also higher than that of MoS_2 as reported before. The consistence of experiments and calculation indicate that $MoSe_2$ has potential to be a better HER catalyst than MoS_2.

Reference

1. Liu, X. Y. Heterogeneous nucleation or homogeneous nucleation? *J. Chem. Phys.* **2000**, *112*, 9949 -9956.

2. Hammer, B.; Hansen, L. B.; Nørskov, J. K. Phys. Rev. B. 1999, 59, 7413.

3. a) G. Kresse , J. Furthmüller , Phys. Rev. B 1996 , 54 , 11169 ; b) G. Kresse , J. Hafner , Phys. Rev. B 1993 , 48 , 13115 ; c) G. Kres ,D. Joubert , Phys. Rev. B 1999 , 59 , 1758 .

4. Berit Hinnemann, Poul Georg Moses, Jacob Bonde, Kristina P. Jørgensen, Jane H. Nielsen, Sebastian Horch, Ib Chorkendorff, Jens K. Nørskov, J. Am. Chem. Soc. 2005, 127, 5308-5309

5. Th. Böker, R. Severin, A. Müller, C. Janowitz, R. Manzke, D. Voβ, P. Krüger, A. Mazur, and J. Pollmann, Phys. Rev. B.2001, 64, 235305.

6. Atkins, P. W. Physical Chemistry, Oxford University Press: Oxford, 1998.